RESEARCH ARTICLE

Adenylate Charge Regulates Sensor Kinase $CheS_3$ To Control Cyst Formation in *Rhodospirillum centenum*

Kuang He,* Vladimira Dragnea, Carl E. Bauer

Molecular and Cellular Biochemistry Department, Indiana University, Bloomington, Indiana, USA

* Present address: Kuang He, ExxonMobil Research and Engineering Company, Annandale, New Jersey, USA.

ABSTRACT ***Rhodospirillum centenum*** **forms metabolically dormant cysts under unfavorable growth conditions such as desiccation or nutrient starvation. The development of cysts is tightly regulated and involves a cyst-repressing chemotaxis-like signal transduction pathway called the Che_3 signaling cascade. The Che_3 cascade is comprised of a methyl chemoreceptor (MCP_3), receptor-methylating/demethylating proteins $CheB_3$ and $CheR_3$, two $CheW_3$ linker proteins, a $CheA_3$-CheY hybrid histidine kinase, and a single-domain response regulator, $CheY_3$. In addition to Che-like components, the Che_3 cascade also contains a second hybrid histidine kinase, $CheS_3$. Recent biochemical and genetic studies show that $CheA_3$ does not serve as a phosphor donor for $CheY_3$; instead, $CheA_3$ inhibits a $CheS_3 \rightarrow CheY_3$ two-component system by phosphorylating an inhibitory receiver domain of $CheS_3$. In this study, we show that in addition to phosphorylation by $CheA_3$, the phosphorylation state of $CheS_3$ is also regulated by the cellular energy level as quantified by the molar ratio of ATP/(ATP + ADP). A 35% decrease in cellular energy is shown to occur *in vivo* upon a nutrient downshift that gives rise to cyst formation. When this energy decline is replicated *in vitro*, the phosphorylation level of $CheS_3$ is reduced by ~75%. Finally, we also show that ADP-mediated reduction of $CheS_3$ phosphorylation is a consequence of ADP enhancing autodephosphorylation of $CheS_3$.**

IMPORTANCE Upon starvation, *Rhodospirillum centenum* undergoes a developmental process that forms metabolically dormant cysts, which withstand desiccation and nutritional limitation. This study explores the role of the cellular energy state as measured by the ratio of ATP to ADP as an important regulator of cyst formation in *Rhodospirillum centenum*. We show that *R. centenum* cells experience a significant reduction in ATP during cyst formation using ATP/(ATP + ADP) as a measurement. When this *in vivo* level of energy starvation is simulated *in vitro*, $CheS_3$ phosphorylation is reduced by 75%. This profound reduction in $CheS_3$ autophosphorylation is contrasted with a much lower 25% decrease in $CheA_3$ phosphorylation in response to a similar downward shift in ATP/(ATP + ADP). We argue that even though adenylate energy affects all ATP-dependent enzymes to an extent, the enhanced inhibition of $CheS_3$ activity in response to a reduction in the ATP/(ATP + ADP) ratio likely functions as an important input signal to regulate cyst development.

Received 1 April 2015 **Accepted** 6 April 2015 **Published** 5 May 2015

Citation He K, Dragnea V, Bauer CE. 2015. Adenylate charge regulates sensor kinase $CheS_3$ to control cyst formation in *Rhodospirillum centenum*. mBio 6(3):e00546-15. doi: 10.1128/mBio.00546-15.

Editor Caroline S. Harwood, University of Washington

Address correspondence to Carl Bauer, Bauer@indiana.edu.

This article is a direct contribution from a Fellow of the American Academy of Microbiology.

Rhodospirillum centenum is a photosynthetic alphaproteobacterium that is also a member of the *Azospirillum* clade (1–4). Members of this clade exhibit a complex life cycle manifested as individual rod- or vibrio-shaped vegetative cells that can differentiate into metabolically dormant round clusters of cells during times of nutrient deprivation or desiccation (3, 5, 6). *Rhodospirillum* and *Azospirillum* constitute part of the plant root rhizosphere, where they are known to provide plants with fixed nitrogen and several plant growth hormones that they synthesize (7–9). Inoculation of seeds with *Azospirillum* species is known to enhance crop yields in a wide variety of cultivars (8, 10).

Unlike extensive analysis of sporulation by Gram-positive cells, little is known about how Gram-negative cells regulate development of metabolically dormant cysts. Recently, we have been studying *R. centenum*, which is a genetically amendable model organism for cyst development by members of the *Azospirillum* clade (5, 11, 12). Genetic studies have indicated that the control of cyst cell development is quite complex, involving numerous histidine kinases, cell cycle regulators, a sigma factor, and the use of cGMP as a signaling molecule (11–15). One of the better-studied regulatory components is a novel Che-like signal transduction cascade (the Che_3 cascade) that controls the timing of cyst development (12, 16). This signal transduction cascade, representing a variation of the classic chemotaxis signaling pathway (17), contains homologs to a methyl chemoreceptor protein (MCP_3), a methyltransferase CheR ($CheR_3$), a methylesterase CheB ($CheB_3$), two linker CheWs ($CheW_{3a}$ and $CheW_{3b}$), a CheA-CheY hybrid histidine kinase ($CheA_3$), and a standalone CheY response regulator/receiver ($CheY_3$) (Fig. 1). By analogy to the *Escherichia coli* chemotaxis signaling paradigm (18), $CheA_3$ is thought to dock

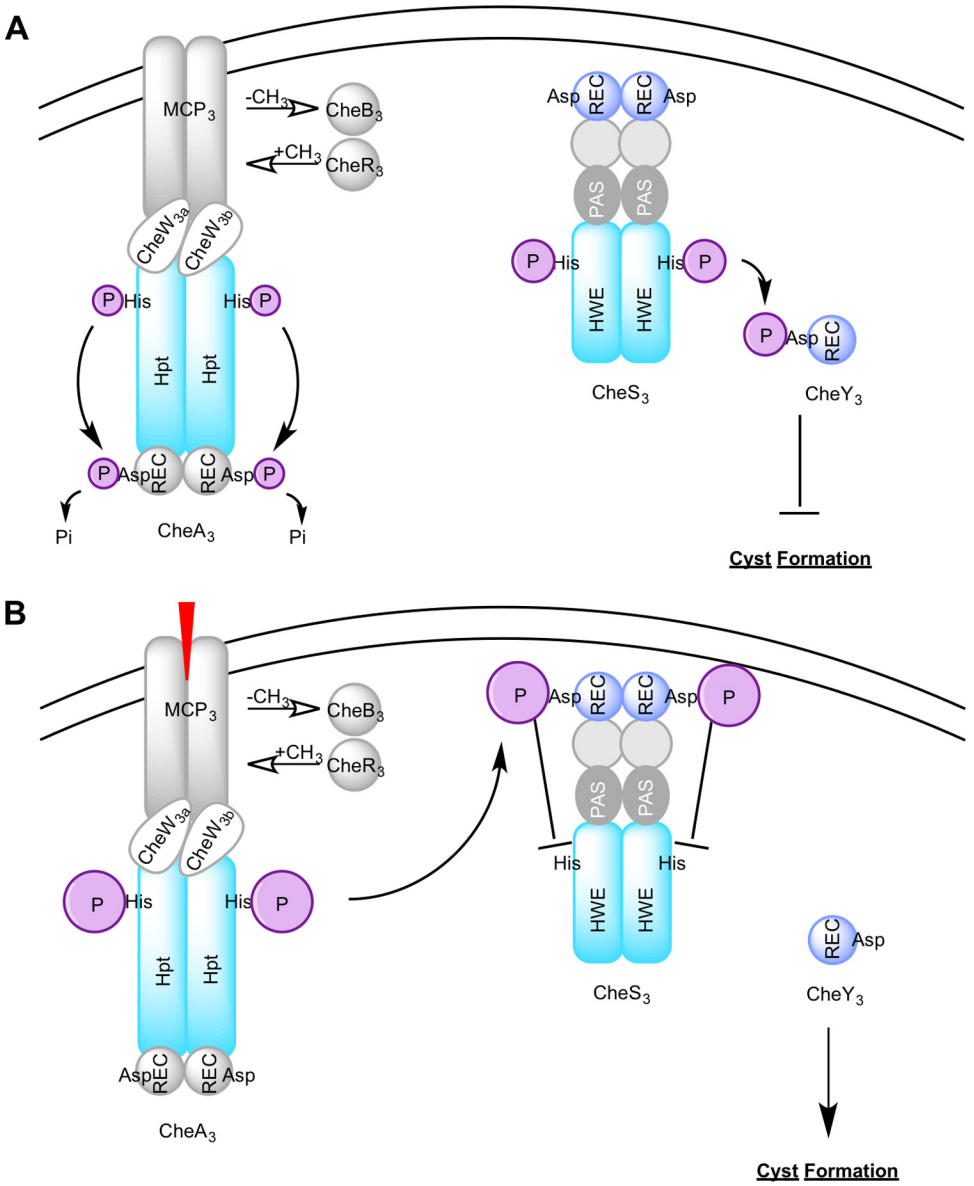

FIG 1 The Che3 signal transduction cascade that controls cyst development. (A) $CheS_3$ and $CheY_3$ comprise a two-component system that is phosphorylated under favorable growth conditions. (B) During the vegetative-to-dormant transition, $CheA_3$ is activated by an external signal (indicated by a red wedge) via the chemoreceptor MCP_3 and phosphorylates the receiver domain of $CheS_3$. When the REC domain is phosphorylated by CheA, it inactivates the ability of the HWE domain to autophosphorylate, thereby deactivating the $CheS_3$-$CheY_3$ two-component system. Abbreviations: REC, receiver domain; PAS, Per-Arnt-Sim domains; HWE, HWE superfamily of histidine kinases; Hpt, histidine phosphotransfer domain.

with $CheW_{3a}$-$CheW_{3b}$, with its kinase activity regulated through signals received by MCP_3. The *che*$_3$ gene cluster also codes for a second hybrid histidine kinase, $CheS_3$, which contains two N-terminal receiver (REC) domains followed by a Per-Arnt-Sim (PAS) domain and an N-terminal HWE class kinase domain. Genetic characterization of the *che*$_3$ gene cluster showed that *cheA*$_3$ null mutants exhibited a defect in cyst formation while *cheS*$_3$ and *cheY*$_3$ null mutants constitutively formed cysts (19). We recently demonstrated that $CheS_3$ and $CheY_3$ constitute a two-component system (TCS) and that under cyst-inducing conditions the kinase activity of $CheS_3$ is inhibited by phosphorylation of the first receiver (REC) domain in $CheS_3$ by $CheA_3$ (12).

Even though autophosphorylation activity of $CheS_3$ is known to be regulated by $CheA_3$ phosphorylation, there remains the possibility that $CheS_3$ may also be regulated by additional intracellular signals. In this report, we demonstrate that the level of $CheS_3$ phosphorylation is indeed fine-tuned by the relative molar ratio of ATP and ADP as explained by the adenylate energy charge (AEC) theory put forth in the late 1960s by Atkinson and Walton (20). AEC is a measure of intracellular energy level based on the amount of high-energy chemical bonds present in ATP and ADP [AEC = (ATP + 1/2 ADP)/(ATP + ADP + AMP)] (20). Cells appear to sustain vegetative growth by maintaining a narrow range of high-energy charge (high ATP relative to ADP and AMP). They do so by regulating the activity of many ATP-utilizing enzymes through inhibition by ADP and/or AMP (21). Since AMP is known to have

a regulatory effect on only eukaryotic serine/threonine protein kinases (22), ATP and ADP are thought to be the key components that affect energy charge in bacterial cells. Interestingly, ATP depletion is a characteristic of a dormant energy-starving state in bacteria (23, 24). For example, sporulating cells such as *Bacillus megaterium* contain strikingly low ATP concentrations relative to vegetatively grown cells (3 nmol ATP/g [dry weight] of spores versus 725 nmol ATP/g [dry weight] of cells) (23). Since nutrient deprivation is one of the triggers for inducing cyst formation (2), we have investigated whether there is a reduction in intracellular energy state as represented by changes in the ratios of adenine nucleotides as *R. centenum* develops cysts. Here, we report that ATP levels are indeed significantly reduced as cells enter dormancy and that $CheS_3$ phosphorylation is also regulated *in vitro* by the ATP/ADP ratio. These results suggest that a reduction in cellular energy charge may constitute an additional regulatory signal for the promotion of encystment.

RESULTS

ATP decreases relative to ADP during encystment. Bacteria typically maintain an AEC between 0.8 and 0.9 during vegetative growth, where high levels of ATP production are sustained (20, 25, 26). However, AEC is reduced in cells entering stationary phase or dormancy, due to nutrient deprivation that limits ATP production. For example, it has been reported that *E. coli* reduces its AEC from 0.92 during logarithmic growth to 0.45 during stationary phase (21). Actively growing *Bacillus megaterium* cells maintain an AEC above 0.79, while stationary pre-sporulation-phase *Bacillus* has a reported AEC of 0.36 and spores of several *Bacillus* species have AEC values below 0.1 (21). We argue that under nutritional starvation, *R. centenum* cells should experience similar ATP depletion that would result in a substantial decline in AEC. Since to our knowledge AMP does not have any known regulatory effects on enzymes of bacterial origin, we evaluated the AEC of *R. centenum* by measuring the ATP/(ATP + ADP) ratio using a luciferase-based ATP luminescence assay. For this analysis, we first grew *R. centenum* in nutrient-rich CENS medium and then shifted the cells into nutrient-limiting CENBA medium to induce encystment (2). Aliquots of the culture were removed at various time points, rapidly disrupted by perchloric acid, and analyzed for adenylate nucleotide pool levels. As shown in Fig. 2A, the intracellular ATP/(ATP + ADP) ratio remained fairly constant at approximately 85% for the first 30 h poststarvation. Within 48 h of growth in CENBA medium, ATP/(ATP + ADP) dropped to approximately 55%, which was sustained for the next 3 days as the cysts matured. Microscopic visual signs of cyst formation (i.e., the formation of highly retractile round cells forming multicell clusters) occurred on day 4.

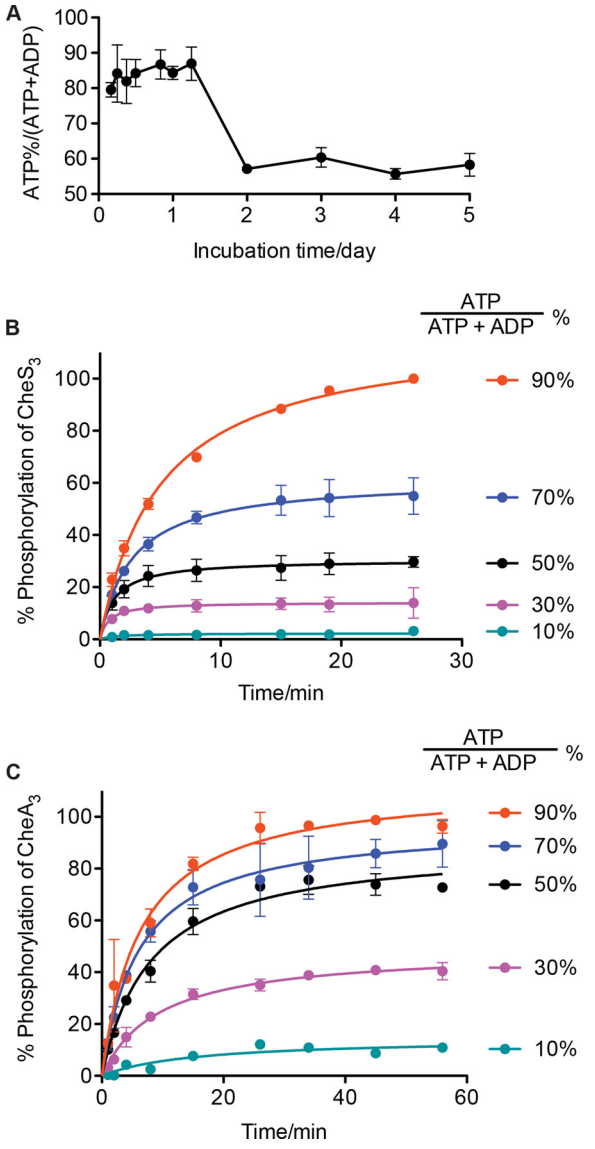

FIG 2 Changes in ATP/(ATP + ADP) observed in encysting *R. centenum* cells affect kinase phosphorylation levels *in vitro*. (A) *In vivo* changes in ATP/(ATP + ADP) in cells experiencing nutrient limitation. Within the first 30 h of incubation, cells propagate at ~85% intracellular ATP/(ATP + ADP), which then drops to ~55% in the next 18 h and maintains the low level in the following 3 days. (B) $CheS_3$ ^{33}P labeling is highly sensitive to changes in ATP/(ATP + ADP) ratios. (C) $CheA_3$ ^{33}P labeling is minimally affected within the 90% to 50% ATP/(ATP + ADP) range. One hundred percent phosphorylation is set to the maximum ^{33}P labeling observed for the duration of the experiments. The error bars represent standard deviations from three replicates.

$CheS_3$ has a lower binding affinity to ATP than does $CheA_3$. Analysis of the intracellular nucleotide concentrations in *E. coli* indicates that logarithmically growing cells typically contain ~3 mM ATP and ~110 μM ADP (27). As discussed above, these levels change as cells transition from logarithmic to stationary phase, with ATP dropping to ~1 mM and ADP increasing to ~400 μM. To address whether similar changes in intracellular nucleotide concentration would equally affect the activity of $CheS_3$ and $CheA_3$, we measured the substrate binding constant for nonhydrolyzable ATPγS and of ADP to both $CheS_3$ and $CheA_3$ using microscale thermophoresis. This technique measures the mobility of molecules in a temperature gradient that depends on molecular weight as well as structural or conformational changes in protein as a consequence of ligand binding. The results of this analysis (Fig. 3) indicate that $CheS_3$ has a significant 8-fold-lower affinity toward ATPγS than does $CheA_3$ (112 nM versus 13 nM, respectively). These values indicate that both kinases should be fully saturated with ATP during logarithmic and stationary phases of growth; however, under severe starvation conditions, as would be expected in metabolically dormant cyst cells, the activity of $CheS_3$ may be selectively inhibited due to its low ATP binding affinity. In the case of ADP, we observed that the two kinases were

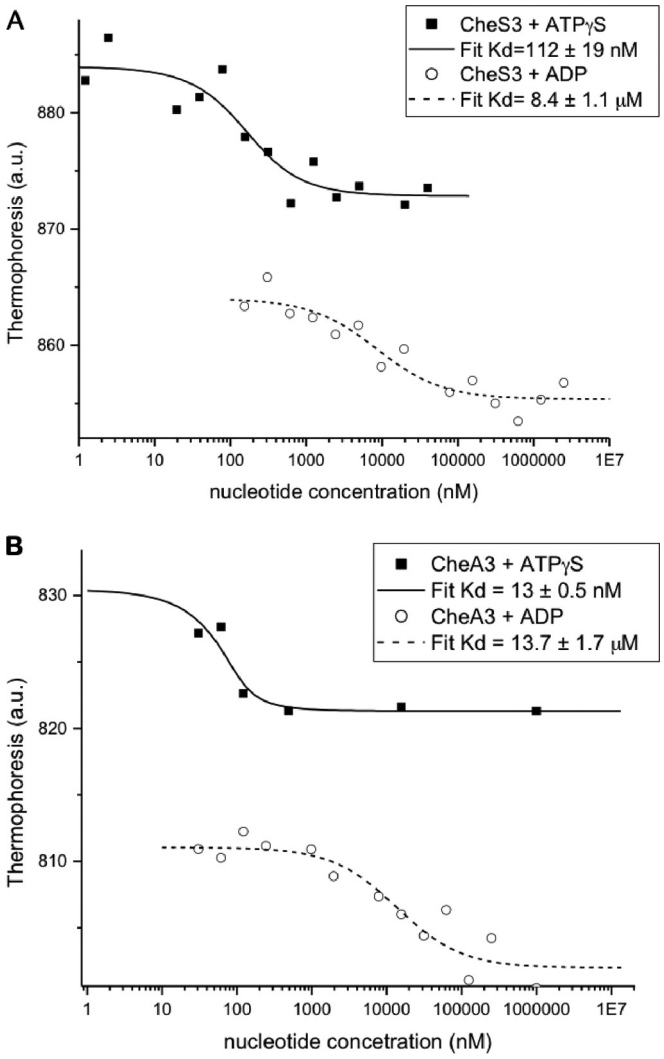

FIG 3 Kinase-nucleotide binding assays using microscale thermophoresis. Increasing concentrations of ATPγS and ADP were incubated with fluorescently labeled $CheS_3$ (A) and $CheA_3$ (B). The thermophoresis signal (a fluorescence "jump" between two states—laser off versus laser on—as a result of movement of fluorescently labeled protein away from the heat spot) was plotted against nucleotide concentrations. Dissociation constant (K_d) values were fitted with sigmoidal binding curves using NanoTemper software.

indeed capable of binding ADP with similar binding constants (8 μM and 14 μM, respectively) (Fig. 3).

Phosphorylation of $CheS_3$ is highly sensitive to elevated ADP concentrations. It has been proposed elsewhere that a reduction in AEC that occurs during starvation could itself function as a metabolic regulator (28). The reason for this conclusion is that an alteration in AEC is known to affect the activity of several ATP-utilizing and ATP-generating enzymes (25). For example, the activity of phosphofructokinase in *E. coli* that controls the flux of metabolites in glycolysis is inhibited by high levels of ATP and stimulated by high levels of ADP (29). Consequently, we investigated whether the *in vitro* kinase activity of $CheS_3$ and $CheA_3$ could be affected by a 30% decrease in ATP/(ATP + ADP) ratio as is observed during a nutrient downshift of *R. centenum* cells. To replicate high, medium, and low ATP/ADP ratios, we formulated a series of ATP/ADP mixes containing a fixed amount of ATP with ADP at various concentrations to achieve ATP/(ATP + ADP) ratios that varied between 90% and 10%. $CheS_3$ and $CheA_3$ were allowed to autophosphorylate in the presence of these ATP/ADP mixes, and the amounts of ^{33}P labeling representing the overall phosphorylation of the kinases were then compared. Figure 2B shows that the level of $CheS_3$ phosphorylation at each time point drops with decreasing ATP/(ATP + ADP) ratios. A profound 70.3% reduction in overall $CheS_3$ phosphorylation at 26 min was observed when the ATP/(ATP + ADP) ratio was decreased from 90% to 50%. This level of reduction in the ATP/(ATP + ADP) ratio is similar to that observed when cells are shifted to the cyst-inducing medium. At an ATP/(ATP + ADP) ratio of 30%, $CheS_3$ contains only 10% ^{33}P incorporation compared to the amount of ^{33}P incorporation observed when ATP/(ATP + ADP) was fixed at 90% (Fig. 2B). When the ADP concentration further increased such that the ATP/(ATP + ADP) was at 13.9%, then $CheS_3$ autophosphorylation was essentially deactivated (Fig. 2B).

We next tested whether ADP inhibition of kinase activity was a characteristic feature of $CheS_3$ or whether it was a general feature of histidine kinases. To address this, we also assayed $CheA_3$'s sensitivity to changes in ATP/(ATP + ADP). As shown in Fig. 2C, $CheA_3$ phosphorylation is also ADP sensitive. However, in contrast to $CheS_3$, ^{33}P labeling of $CheA_3$ is only slightly diminished (23.9%) by a similar 90% to 50% decrease in the ATP/(ATP + ADP) ratio at 57 min (Fig. 2C). $CheA_3$ starts to exhibit a greater reduction in overall phosphorylation as ATP/(ATP + ADP) drops below 50%.

ADP affects the stability of phosphorylated $CheS_3$. Since $CheS_3$ exhibits an unusually sensitive response to changes in the adenylate energy state as measured by ATP/(ATP + ADP), we next investigated the role of ADP in regulating $CheS_3$. One possibility is that an excessive amount of ADP occupies and blocks the active site, preventing the enzyme from autophosphorylating. Another hypothesis is that ADP drives the reverse reaction of autophosphorylation to form ATP. It is also possible that ADP boosts the intrinsic hydrolysis of the phosphohistidine bonds or promotes intramolecular phosphoryl transfer to its REC1 domain, which is known to undergo rapid autodephosphorylation. We tested these possibilities by first assessing the stability of purified $CheS_3$~P in the presence of ADP, ATP, or AMP. For this analysis, we first autophosphorylated $CheS_3$ at room temperature for 30 min with excess [^{33}P]ATP and then removed unincorporated ATP with a desalting column. Isolated $CheS_3$~P was then exposed to 100 μM ATP, ADP, or AMP and then assayed for phosphate stability by SDS-PAGE analysis. The results shown in Fig. 4A indicate that exposure of $CheS_3$~P to 100 μM ADP resulted in greatly accelerated dephosphorylation (half-life of 0.02 min) relative to the stability observed in the presence of ATP and AMP (half-life of 53 min) or in the absence of any nucleotides (55.4 min) (12).

We next analyzed the nature of the products formed as a result of ADP destabilization using thin-layer chromatography (Fig. 4B). $CheS_3$~P was immobilized onto Ni^{2+}-Sepharose resin and rinsed 5 times with buffer before 100 μM ADP was introduced. The purification step was not thorough, as a trace amount of ATP was still present at the 20-s time point (Fig. 4B). However, ATP disappeared at the 40-s time point, indicating that despite excess ADP, ATP was still hydrolyzed presumably by $CheS_3$ in an autophosphorylation event. Additionally, $CheS_3$~P, which should remain at the origin, also disappeared at 40 s, suggesting that the

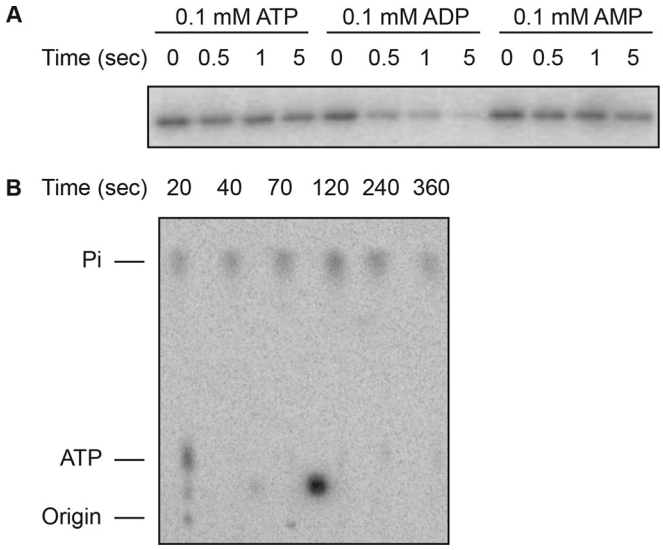

FIG 4 The stability of phosphorylated $CheS_3$ is greatly reduced in the presence of ADP. (A) Purified $CheS_3$~P dephosphorylates within 30 s in the presence of 0.1 mM ADP, which was not observed with the same concentrations of ATP or AMP. (B) ADP drives dephosphorylation of $CheS_3$~P to form inorganic phosphates (P_i) as assayed by thin-layer chromatography (TLC).

phosphoprotein had released its phosphoryl group. Since no ATP was reformed beyond 40 s, ADP does not drive the reverse reaction of autophosphorylation. Finally, ADP does not promote intramolecular transfer of phosphates from the HK domain to the REC1 domain, as the phosphorylated form of $CheS_3$ and its nonphosphorylatable REC domain mutant $CheS_3$:D54A are both base resistant in the presence of ADP (Fig. 5). These results suggest that ADP interacts with $CheS_3$~P in a manner that leads to destabilization of the phosphor-histidine bond.

DISCUSSION

While a nutrient downshift seems to initiate the formation of resting cells in many bacterial species, the actual signals that regulate the development of dormancy remain unclear. For example, the multicomponent Spo0F-Spo0B-Spo0A phosphorelay that controls sporulation in *Bacillus subtilis* involves three sensor kinases: KinA and KinB, which phosphorylate Spo0F (30), and KinC, which directly phosphorylates the DNA binding response regulator Spo0A (31). The only clue that might reveal the input signal for these sporulation kinases is that the transmembrane kinase KinC responds to small-molecule natural products that cause potassium leakage from the cytosol (32). However, it remains unclear what input signals are actually being sensed by KinA and KinB.

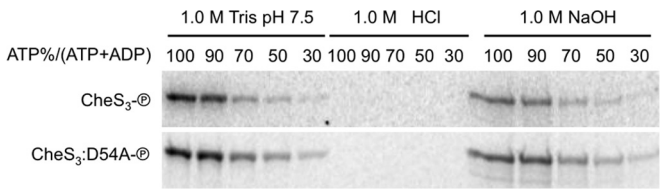

FIG 5 Acid-base stability test of $CheS_3$ and its receiver mutant. Autophosphorylation was carried out in the presence of 100%, 90%, 70%, 50%, and 30% ATP/(ATP + ADP). Under these conditions, both phosphorylated $CheS_3$ and $CheS_3$:D54A are acid labile and alkaline stable, suggesting that both forms of $CheS_3$ are phosphorylated only at the conserved histidine site despite the varied adenylate energy levels.

In this report, we propose that $CheS_3$ responds to alterations in ATP/ADP ratios upon starvation. The intracellular ATP-to-ADP ratio has previously been shown to be sufficient to entrain circadian oscillators reconstituted *in vitro* with isolated cyanobacterial kinases (33). In this case, light illumination drives *in vivo* oscillations of ATP/ADP ratios, which in turn generate a circadian KaiC oscillator where the phosphorylation of KaiC is regulated by two other proteins, KaiA and KaiB. Furthermore, darkness induces a phase shift of the KaiABC system, which can be simulated *in vitro* by lowering the ATP/ADP ratios alone. Here, we show that a nutrient downshift causes a decrease in the ATP/ADP ratio in *R. centenum* cells and that changes in the ATP/ADP ratio similar to those that occur during cyst formation modulate $CheS_3$ phosphorylation levels *in vitro*. In response to the measured 35% drop between the initial high and final low ATP/(ATP + ADP) ratios that occurs upon a nutrient downshift, the $CheS_3$ phosphorylation level is reduced by approximately 75% relative to its peak level. This 35% drop in the ATP pool relative to the total amount of ATP and ADP could be an underestimate due to samples containing a mixed population of mature cysts and cells that have not proceeded entirely through the encystment process. So, there is a possibility that $CheS_3$ can be deactivated even more than what we have observed. The great sensitivity of $CheS_3$~P to fluctuations in the ATP/ADP ratio during encystment is distinct from moderate resistance exhibited by $CheA_3$~P. As ATP/(ATP + ADP) drops from the vegetative level to the dormant level, $CheA_3$ loses only 25% of its phosphorylation. This difference in inhibition by these two sensor kinases may at one level be due to differences in the ATP binding affinities of $CheA_3$ and $CheS_3$. $CheA_3$ binds ATP 8-fold more tightly and therefore remains more active in utilizing ATP even at ultralow ATP intracellular concentrations that would occur during cyst formation. Furthermore, $CheA_3$ phosphorylation of the Rec1 domain of $CheS_3$ is known to inhibit the formation of a phosphor-histidine bond in $CheS_3$. Thus, a sharp step down in ATP levels would favor this inhibition event, as $CheA_3$ is more resistant to a reduction in ATP levels, allowing it to continue to phosphorylate Rec1 in $CheS_3$. In fact, the ATP binding affinity for $CheA_3$ is about 2 to 200 times higher than that reported for other histidine kinases (34–37). This tight binding ensures that $CheA_3$ remains active even during the energy starvation periods. We further demonstrate that ADP stimulates hydrolysis of $CheS_3$~P to generate P_i by affecting the stability of the phosphohistidine bond. We speculate that when ADP builds up during a nutrient downshift, any phosphohistidine present on $CheS_3$ is rapidly removed by ADP-stimulated dephosphorylation (Fig. 6). To our knowledge, this is a novel mechanism of dephosphorylation not described for other histidine kinases.

Gram-negative cysts are nonreplicative dormant cells like that of dormant Gram-positive spores. In both cases, there appear to be many input signals and checkpoints harbored by these cells to regulate these developmental processes so as to ensure that the cell enters a nonreplicative survival pathway only when conditions for survival are harsh. The inputs to control *Rhodospirillum/Azospirillum* Gram-negative encystment are complex, involving production of cGMP (11), the complex Che_3 signaling cascade (12, 17, 19), and the cellular energy charge. In the Gram-positive bacterium *Bacillus subtilis*, there are many histidine sensor kinases (KinA, KinB, KinC, KinD, and KinE) that are involved in controlling the decision to induce encyst-

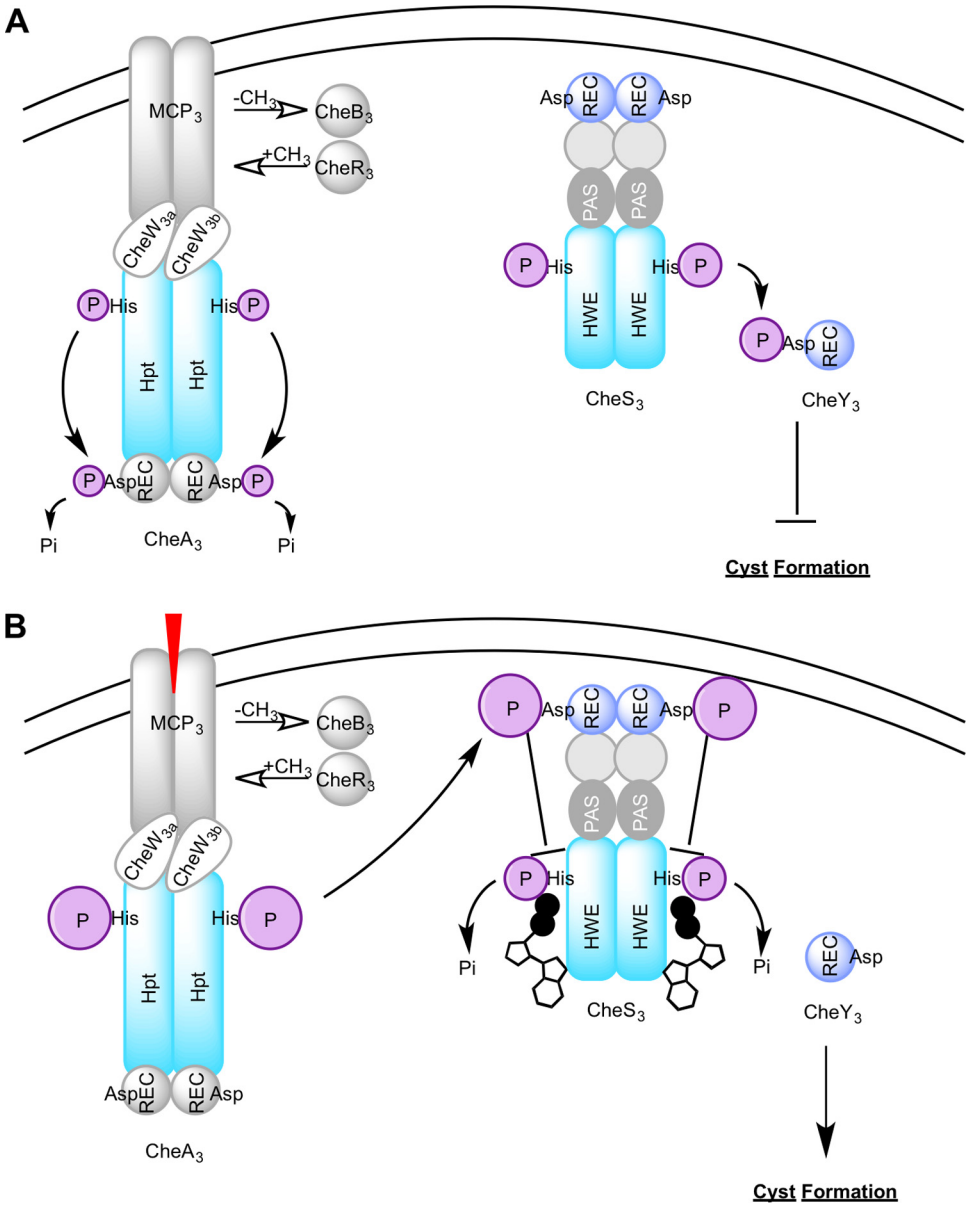

FIG 6 Revised Che_3 signal transduction cascade under the control of adenylate energy charge. (A) During vegetative growth, the $CheS_3$-$CheY_3$ two-component system is active at high intracellular ATP/ADP ratios. (B) Upon energy starvation, ATP is quickly depleted and ADP (indicated by the molecular mechanism) is accumulated, leading to dephosphorylation of the HK domain of $CheS_3$; in the meantime, $CheA_3$ is activated by an external signal (indicated by a red wedge) via the chemoreceptor MCP_3 and inhibits the $CheS_3$ kinase activity by phosphorylating its receiver domain.

ment (31, 38–41). Despite years of study, it remains unclear what signal most of these kinases receive to control their autophosphorylation activity. Although untested, it is possible that the cellular energy charge may also be an input that affects one or more Kin kinase activities so as to induce sporulation at times when the cells are undergoing a drop in energy production.

MATERIALS AND METHODS

Overexpression and purification of $CheS_3$ and $CheA_3$. $CheS_3$ and $CheA_3$ were overexpressed in *E. coli* BL21 Rosetta 2(DE3) cells (Novagen) and isolated as previously described (12).

Kinase assays. Kinase assays for $CheS_3$ utilized buffer S (25 mM Tris-HCl, pH 7.4, 100 mM NaCl, 3 mM $MgCl_2$, 3 mM $CaCl_2$, 10% glycerol), and those for $CheA_3$ utilized buffer A (25 mM Tris-HCl, pH 7.4, 100 mM KCl, 6 mM $CaCl_2$, 10% glycerol). Protein freezer stocks were diluted in the appropriate buffers to yield 2 to 5 μM working aliquots for $CheS_3$ and $CheA_3$. For ATP/ADP ratio experiments, a series of radioactive ATP/ADP solutions was prepared by mixing fixed amounts of [γ-^{33}P]ATP (>3,000 Ci/mmol; PerkinElmer) and unlabeled ATP with varied amounts of ADP to achieve 0.8 mM total ATP with ATP/(ATP + ADP) ranging from 10% to 90%. Autophosphorylation was initiated at room temperature by adding 1 volume of ATP/ADP mix to 3 volumes of $CheS_3$ or $CheA_3$. For all kinase assays, reaction aliquots were removed and reactions were stopped by mixing with 6× SDS-PAGE sample loading buffer. Protein samples were subjected to SDS-PAGE, and gels were examined by autoradiography on a Typhoon 9100 scanner (GE Healthcare). Phosphorylation of the kinases was quantified using ImageJ by integrating the grayscale density of the radioactive bands.

Nucleotide extraction and ATP and ADP determination. Cells from overnight cultures were washed two times with 40 mM phosphate buffer and inoculated in CENBA medium at a 1:40 ratio. These subcultures were aliquoted 3 ml/test tube and shaken at 37°C. At each time point, 675 μl of chilled 3 M perchloric acid and 75 μl of chilled 500 mM EDTA (pH 8.0) were simultaneously added into each tube. The acid-treated cultures were quickly shaken and placed on ice. Cell lysis was performed using FastPrep with Lysis Matrix B (MP Biomedicals), and cell debris was cleared by centrifugation at 13,000 rpm for 10 min. The supernatant was then neutralized with a solution of 1 M Tris-HCl, 0.5 M KOH, and 0.5 M KCl to pH 7.5. $KClO_4$ precipitate was removed by centrifugation, and the nucleotide extracts were diluted in 20 mM Tris-HCl, pH 7.5, containing 2 mM EDTA before storage at −80°C. The ATP/(ATP + ADP) ratios were determined using a commercial bioluminescence-based assay kit (EnzyLight; Bioassay Systems).

Measurement of ADP and ATP binding constants with microscale thermophoresis. $CheS_3$ protein (20 μM) was fluorescently labeled using the Monolith NT protein labeling kit Blue-NHS (NanoTemper Technologies) according to the manufacturer's instructions. Labeled protein was diluted to 100 nM, mixed with 16 increasing concentrations of ADP or ATPγS (various ranges were tested to optimize the signal), incubated for a short period, and transferred into 16 standard capillaries. Thermophoresis measurements were performed using a Monolith N-115 (NanoTemper Technologies) and automated Monolith data acquisition software. Data were fitted using the standard temperature jump and thermophoresis model using NanoTemper analysis software.

ADP stability assays. Three aliquots of 10 μM $CheS_3$ were allowed to autophosphorylate at room temperature for 30 min, with excess ATP and [γ-^{32}P]ATP subsequently being removed by filtration using Zeba spin desalting columns (Thermo Scientific). Forty-five microliters of each aliquot was mixed with 30 μl of buffer 5 (12) to which 15 μl of 1 mM ATP, ADP, or AMP was added and then incubated at room temperature for 15 min. Protein samples were subjected to SDS-PAGE and autoradiography.

Thin-layer chromatography (TLC). $CheS_3$~P was immobilized onto Ni^{2+}-Sepharose resin and rinsed 5 times with buffer, and $CheS_3$~P-loaded resin was suspended in 100 μM ADP at time zero. Aliquots of the resin suspension were treated with equal volumes of 1 M formic acid before spotting on polyethyleneimine cellulose plates, which were then developed in 0.75 M KH_2PO_4, pH 3.75.

Acid-base stability assays. The $CheS_3$ phosphorylation state was determined by assaying phosphoprotein stability after autophosphorylation in the presence of acids, Tris buffer, or bases as previously described (12).

ACKNOWLEDGMENT

Funding for this study was provided by a National Institutes of Health grant GM099703 to C.E.B.

REFERENCES

1. **Favinger J, Stadtwald R, Gest H.** 1989. *Rhodospirillum centenum*, sp. nov., a thermotolerant cyst-forming anoxygenic photosynthetic bacterium. Antonie Van Leeuwenhoek **55:**291–296. http://dx.doi.org/10.1007/BF00393857.
2. **Stadtwald-Demchick R, Turner FR, Gest H.** 1990. Physiological properties of the thermotolerant photosynthetic bacterium, *Rhodospirillum centenum*. FEMS Microbiol Lett **67:**139–143. http://dx.doi.org/10.1111/j.1574-6968.1990.tb13851.x.
3. **Nickens D, Fry CJ, Ragatz L, Bauer CE, Gest H.** 1996. Biotype of the purple nonsulfur photosynthetic bacterium, *Rhodospirillum centenum*. Arch Microbiol **165:**91–96. http://dx.doi.org/10.1007/s002030050302.
4. **Stoffels M, Castellanos T, Hartmann A.** 2001. Design and application of new 16S rRNA-targeted oligonucleotide probes for the *Azospirillum-Skermanella-Rhodocista*-cluster. Syst Appl Microbiol **24:**83–97. http://dx.doi.org/10.1078/0723-2020-00011.
5. **Berleman JE, Bauer CE.** 2004. Characterization of cyst cell formation in the purple photosynthetic bacterium *Rhodospirillum centenum*. Microbiology **150:**383–390. http://dx.doi.org/10.1099/mic.0.26846-0.
6. **Sadasivan L, Neyra CA.** 1987. Cyst production and brown pigment formation in aging cultures of *Azospirillum brasilense* ATCC 29145. J Bacteriol **169:**1670–1677.
7. **Steenhoudt O, Vanderleyden J.** 2000. *Azospirillum*, a free-living nitrogen-fixing bacterium closely associated with grasses: genetic, biochemical and ecological aspects. FEMS Microbiol Rev **24:**487–506. http://dx.doi.org/10.1111/j.1574-6976.2000.tb00552.x.
8. **Bashan Y, de-Bashan LE.** 2010. How the plant growth-promoting bacterium *Azospirillum* promotes plant growth—a critical assessment. Adv Agron **108:**77–136. http://dx.doi.org/10.1016/S0065-2113(10)08002-8.
9. **Fibach-Paldi S, Burdman S, Okon Y.** 2012. Key physiological properties contributing to rhizosphere adaptation and plant growth promotion abilities of *Azospirillum brasilense*. FEMS Microbiol Lett **326:**99–108. http://dx.doi.org/10.1111/j.1574-6968.2011.02407.x.
10. **Okon Y, Labandera-Gonzalez CA.** 1994. Agronomic applications of *Azospirillum*: an evaluation of 20 years worldwide field inoculation. Soil Biol Biochem **26:**1591–1601. http://dx.doi.org/10.1016/0038-0717(94)90311-5.
11. **Marden JN, Dong Q, Roychowdhury S, Berleman JE, Bauer CE.** 2011. Cyclic GMP controls *Rhodospirillum centenum* cyst development. Mol Microbiol **79:**600–615. http://dx.doi.org/10.1111/j.1365-2958.2010.07513.x.
12. **He K, Marden JN, Quardokus EM, Bauer CE.** 2013. Phosphate flow between hybrid histidine kinases CheA3 and CheS3 controls *Rhodospirillum centenum* cyst formation. PLoS Genet **9:**e1004002. http://dx.doi.org/10.1371/journal.pgen.1004002.
13. **Berleman JE, Hasselbring BM, Bauer CE.** 2004. Hypercyst mutants in *Rhodospirillum centenum* identify regulatory loci involved in cyst cell differentiation. J Bacteriol **186:**5834–5841. http://dx.doi.org/10.1128/JB.186.17.5834-5841.2004.
14. **Bird TH, MacKrell A.** 2011. A CtrA homolog affects swarming motility and encystment in *Rhodospirillum centenum*. Arch Microbiol **193:**451–459. http://dx.doi.org/10.1007/s00203-011-0676-y.
15. **Din N, Shoemaker CJ, Akin KL, Frederick C, Bird TH.** 2011. Two putative histidine kinases are required for cyst formation in *Rhodospirillum centenum*. Arch Microbiol **193:**209–222. http://dx.doi.org/10.1007/s00203-010-0664-7.
16. **Berleman JE, Bauer CE.** 2005. A che-like signal transduction cascade involved in controlling flagella biosynthesis in *Rhodospirillum centenum*. Mol Microbiol **55:**1390–1402. http://dx.doi.org/10.1111/j.1365-2958.2005.04489.x.
17. **He K, Bauer CE.** 2014. Chemosensory signaling systems that control bacterial survival. Trends Microbiol **22:**389–398. http://dx.doi.org/10.1016/j.tim.2014.04.004.
18. **Porter SL, Wadhams GH, Armitage JP.** 2011. Signal processing in complex chemotaxis pathways. Nat Rev Microbiol **9:**153–165. http://dx.doi.org/10.1038/nrmicro2505.
19. **Berleman JE, Bauer CE.** 2005. Involvement of a Che-like signal transduction cascade in regulating cyst cell development in *Rhodospirillum centenum*. Mol Microbiol **56:**1457–1466. http://dx.doi.org/10.1111/j.1365-2958.2005.04646.x.
20. **Atkinson DE, Walton GM.** 1967. Adenosine triphosphate conservation in metabolic regulation. Rat liver citrate cleavage enzyme. J Biol Chem **242:**3239–3241.
21. **Chapman AG, Fall L, Atkinson DE.** 1971. Adenylate energy charge in *Escherichia coli* during growth and starvation. J Bacteriol **108:**1072–1086.
22. **Hardie DG.** 2011. AMP-activated protein kinase: an energy sensor that regulates all aspects of cell function. Genes Dev **25:**1895–1908. http://dx.doi.org/10.1101/gad.17420111.
23. **Setlow P, Kornberg A.** 1970. Biochemical studies of bacterial sporulation and germination. XXII. Energy metabolism in early stages of germination of Bacillus megaterium spores. J Biol Chem **245:**3637–3644.
24. **Loshon CA, Setlow P.** 1993. Levels of small molecules in dormant spores of Sporosarcina species and comparison with levels in spores of *Bacillus* and *Clostridium* species. Can J Microbiol **39:**259–262. http://dx.doi.org/10.1139/m93-036.
25. **Atkinson DE.** 1968. The energy charge of the adenylate pool as a regulatory parameter. Interaction with feedback modifiers. Biochemistry **7:**4030–4034. http://dx.doi.org/10.1021/bi00851a033.
26. **Sakakibara T, Murakami S, Imai K.** 2003. Enumeration of bacterial cell numbers by amplified firefly bioluminescence without cultivation. Anal Biochem **312:**48–56. http://dx.doi.org/10.1016/S0003-2697(02)00427-X.
27. **Buckstein MH, He J, Rubin H.** 2008. Characterization of nucleotide

pools as a function of physiological state in *Escherichia coli*. J Bacteriol **190:**718–726. http://dx.doi.org/10.1128/JB.01020-07.
28. **Atkinson DE**. 1969. Regulation of enzyme function. Annu Rev Microbiol **23:**47–68. http://dx.doi.org/10.1146/annurev.mi.23.100169.000403.
29. **Reeves RE, Sols A**. 1973. Regulation of *Escherichia coli* phosphofructokinase in situ. Biochem Biophys Res Commun **50:**459–466. http://dx.doi.org/10.1016/0006-291X(73)90862-0.
30. **Burbulys D, Trach KA, Hoch JA**. 1991. Initiation of sporulation in *B. subtilis* is controlled by a multicomponent phosphorelay. Cell **64:**545–552. http://dx.doi.org/10.1016/0092-8674(91)90238-T.
31. **LeDeaux JR, Grossman AD**. 1995. Isolation and characterization of *kinC*, a gene that encodes a sensor kinase homologous to the sporulation sensor kinases KinA and KinB in *Bacillus subtilis*. J Bacteriol **177:**166–175.
32. **López D, Gontang EA, Kolter R**. 2010. Potassium sensing histidine kinase in *Bacillus subtilis*. Methods Enzymol **471:**229–251. http://dx.doi.org/10.1016/S0076-6879(10)71013-2.
33. **Rust MJ, Golden SS, O'Shea EK**. 2011. Light-driven changes in energy metabolism directly entrain the cyanobacterial circadian oscillator. Science **331:**220–223. http://dx.doi.org/10.1126/science.1197243.
34. **Shrivastava R, Ghosh AK, Das AK**. 2007. Probing the nucleotide binding and phosphorylation by the histidine kinase of a novel three-protein two-component system from *Mycobacterium tuberculosis*. FEBS Lett **581:** 1903–1909. http://dx.doi.org/10.1016/j.febslet.2007.03.089.
35. **Plesniak L, Horiuchi Y, Sem D, Meinenger D, Stiles L, Shaffer J, Jennings PA, Adams JA**. 2002. Probing the nucleotide binding domain of the osmoregulator EnvZ using fluorescent nucleotide derivatives. Biochemistry **41:**13876–13882. http://dx.doi.org/10.1021/bi020331j.
36. **Surette MG, Levit M, Liu Y, Lukat G, Ninfa EG, Ninfa A, Stock JB**. 1996. Dimerization is required for the activity of the protein histidine kinase CheA that mediates signal transduction in bacterial chemotaxis. J Biol Chem **271:**939–945. http://dx.doi.org/10.1074/jbc.271.2.939.
37. **Nowak E, Panjikar S, Morth** JP, Jordanova R, Svergun DI, Tucker PA. 2006. Structural and functional aspects of the sensor histidine kinase PrrB from *Mycobacterium tuberculosis*. Structure 14:275–285. http://dx.doi.org//10.1016/j.str.2005.10.006.
38. **LeDeaux JR, Yu N, Grossman AD**. 1995. Different roles for KinA, KinB, and KinC in the initiation of sporulation in *Bacillus subtilis*. J Bacteriol **177:**861–863.
39. **Jiang M, Shao W, Perego M, Hoch JA**. 2000. Multiple histidine kinases regulate entry into stationary phase and sporulation in *Bacillus subtilis*. Mol Microbiol **38:**535–542. http://dx.doi.org/10.1046/j.1365-2958.2000.02148.x.
40. **Kobayashi K, Shoji K, Shimizu T, Nakano K, Sato T, Kobayashi Y**. 1995. Analysis of a suppressor mutation *ssb* (*kinC*) of sur0B20 (*spo0A*) mutation in *Bacillus subtilis* reveals that *kinC* encodes a histidine protein kinase. J Bacteriol **177:**176–182.
41. **Tan IS, Ramamurthi KS**. 2014. Spore formation in *Bacillus subtilis*. Environ Microbiol Rep **6:**212–225. http://dx.doi.org/10.1111/1758-2229.12130.